JOURNAL OF COMPUTATIONAL PHYSICS 109, 274–288 (1993)

Explicit Streamline Diffusion Finite Element Methods for the Compressible Euler Equations in Conservation Variables

PETER HANSBO

Department of Mathematics, Chalmers University of Technology, S-412 96 Göteborg, Sweden

Received December 17, 1991; revised September 29, 1992

The paper concerns the streamline diffusion finite element method applied to one- and two-dimensional gas flow described by the inviscid Euler equations in conservation variables. We point out that the streamline diffusion method is a natural finite element analogue to upstream-type finite difference/volume schemes and in fact constitutes a general framework for a large class of them. We study explicit implementations of the method and derive different choices of stabilizing streamline diffusion matrices; in particular we propose a consistent, fully multidimensional, version. A brief review of the theoretical background to the method is presented, and some numerical results in two dimensions are given.

1. INTRODUCTION

The finite element method (FEM) is relatively new in the field of computational fluid dynamics, which has been, and still is, dominated by finite difference methods. With the increase in computational power during the last decade, the possibility of using unstructured meshes to model complex geometries (and the ease with which local refinement of the mesh can be performed) has given rise to a growing interest in FEM. The initial problems of obtaining results for convective problems with this method were due to the fact that the standard Galerkin FEM gives rise to central-difference type schemes that are extremely unstable for convection dominated problems.

The streamline diffusion (SD) finite element method enhances the stability of Galerkin FEM through adding a small least-squares term to the test functions, which, for scalar convection problems, corresponds to adding diffusion in the streamline direction. The SD-method was introduced by Hughes and co-workers in the early eighties and has been developed into a general method for hyperbolic problems, mainly by Hughes and by Johnson, together with their respective co-workers. In the context of compressible flow we refer to, e.g., [1–7].

For time-dependent problems, the SD-method is based on a general space-time finite element mesh, with the basis functions continuous in space but discontinuous in time at discrete time-levels t_n. This is achieved by use of an SD-modification of the time-discontinuous Galerkin method, in which the mesh is organised into space-time "slabs" $S_n = \Omega \times (t_n, t_{n+1})$, where Ω is the underlying spatial domain.

In the paper by Hansbo and Johnson, [7], non-linearly implicit implementations of the SD-method in conservation variables were considered, which yield unnecessarily slow schemes. The purpose of the present paper is twofold: first, we obtain faster schemes by considering explicit versions of the method; second, we point out that the SD-method is a natural FEM-generalization of upstream-type finite difference and finite volume methods. We derive, in the spirit of Hughes *et al.* [1, 2], expressions for the generalizations of the scalar streamline diffusion perturbation, applied to systems of equations, and suggest an explicit stabilizing artificial viscosity term based on the residual of the solution.

An outline of the paper is as follows. In Section 2 we discuss the SD-method applied to general systems of conservation laws equipped with an entropy function and point out the entropy stability obtained with the method. Section 3 concerns explicit methods for the one-dimensional Euler equations and in Section 4 we point out different possibilities for the two-dimensional case. Section 5 contains numerical examples for some two-dimensional problems, and in Section 6 we give some concluding remarks.

2. THE STREAMLINE DIFFUSION METHOD

In this section, we give a brief review of the theoretical background of the SD-method. In particular, we discuss the transition from entropy variables to conservation variables, thus motivating the form of the SD-method in conservation variables.

Symmetric Forms of Conservation Laws

A breakthrough in the formulation of SD-methods for compressible flow came with the idea of using symmetrized conservation laws, introduced and developed by Hughes *et al.* [2, 3, 8]. The symmetrization is accomplished by the introduction of *entropy variables*, given that the conserva-

0021-9991/93 $5.00

tion laws are equipped with an *entropy function*. Consider a system of conservation laws of the form

$$\frac{\partial \mathbf{u}}{\partial t}+\sum_{i=1}^{d}\frac{\partial \mathbf{f}_i(\mathbf{u})}{\partial x_i}=0, \tag{2.1}$$

where $\mathbf{u}$ is a vector of unknowns and the $\mathbf{f}_i$ are vector-valued functions of $\mathbf{u}$. By entropy function is understood a scalar convex function $\eta=\eta(\mathbf{u})$ associated with *entropy flux functions* $q_i=q_i(\mathbf{u})$ such that the relations

$$\left[\frac{\partial \eta}{\partial \mathbf{u}}\right]^{\mathrm{T}}\mathbf{A}_i=\left[\frac{\partial q_i}{\partial \mathbf{u}}\right]^{\mathrm{T}}, \tag{2.2}$$

hold, where

$$\mathbf{A}_i=\mathbf{A}_i(\mathbf{u})=\frac{\partial \mathbf{f}_i}{\partial \mathbf{u}}$$

are the Jacobians of the $\mathbf{f}_i$. Given a set $\{n_i\}$ of arbitrary real numbers (not all zero), we assume that the matrix $\sum_i n_i\mathbf{A}_i$ has real eigenvalues and a complete set of linearly independent eigenvectors, so that (2.1) is a hyperbolic system.

If discontinuities occur in the solution, (2.1) does not define a unique solution, and in order to single out the physically relevant solution (defined as a vanishing viscosity solution) we must have

$$\frac{\partial \eta(\mathbf{u})}{\partial t}+\sum_{i=1}^{d}\frac{\partial q_i(\mathbf{u})}{\partial x_i}\leqslant 0, \tag{2.3}$$

with equality only if the solution is smooth.

As pointed out by Mock [9], the system of conservation laws may be symmetrized by the (invertible) change of variables

$$\mathbf{v}=\mathbf{v}(\mathbf{u})=\partial\eta/\partial\mathbf{u}. \tag{2.4}$$

With this choice of variables, Eq. (2.1) can be written

$$\mathbf{B}_0\frac{\partial \mathbf{v}}{\partial t}+\sum_{i=1}^{d}\mathbf{B}_i\frac{\partial \mathbf{v}}{\partial x_i}=0, \tag{2.5}$$

where

$$\mathbf{B}_0=\frac{\partial \mathbf{u}}{\partial \mathbf{v}}=\left[\frac{\partial^2\eta}{\partial \mathbf{u}^2}\right]^{-1}\qquad\text{and}\qquad \mathbf{B}_i=\mathbf{A}_i\mathbf{B}_0.$$

All of the matrices $\mathbf{B}_j$, $j=0, 1, \ldots, d$, are symmetric. Further discussions and elaborations on the subject of entropy variables can be found in, e.g., [8–11].

The Streamline Diffusion Method in Entropy Variables

To define the SD-method for the approximate solution of (2.5), let $0=t_0<t_1<t_2\cdots$ be a sequence of discrete time-levels t_n, and let S_n denote the space-time "slab" $\Omega\times(t_n, t_{n+1})$, where Ω is the physical domain. We seek an approximate solution

$$\mathbf{V}=\sum_i \mathbf{V}_i\phi_i(\mathbf{x}, t), \tag{2.6}$$

where $\mathbf{x}=(x_1, \ldots, x_d)$, $\mathbf{V}_i$ denotes nodal values of $\mathbf{V}$, and ϕ_i are the space-time finite element basis functions corresponding to the discretization of S_n, continuous in space but discontinuous in time at discrete time-levels. For $n=0, 1, \ldots$, we seek a $\mathbf{V}\simeq\mathbf{v}$ such that

$$\begin{aligned}\int_{S_n}&\left[\mathbf{w}+\mathbf{\Theta}_E\left(\mathbf{B}_0\frac{\partial \mathbf{w}}{\partial t}+\sum_i\mathbf{B}_i\frac{\partial \mathbf{w}}{\partial x_i}\right)\right]^{\mathrm{T}}\\ &\times\left[\mathbf{B}_0\frac{\partial \mathbf{V}}{\partial t}+\sum_i\mathbf{B}_i\frac{\partial \mathbf{V}}{\partial x_i}\right]dS_n\\ &+\int_{\Omega}\mathbf{w}_+^{\mathrm{T}}\mathbf{B}_0(\mathbf{V}_+-\mathbf{V}_-)\,d\Omega=0\end{aligned} \tag{2.7}$$

for all $\mathbf{w}$ that can be written in the form (2.6). Here

$$\mathbf{w}_{\pm}=\lim_{s\to 0+}\mathbf{w}(t_n\pm s),$$

and $\mathbf{\Theta}_E$ is a matrix, the appearance of which has been discussed elsewhere [8, 5]. Note that data is transported from one slab to the next via a built-in projection in the jump term

$$\int_{\Omega}\mathbf{w}_+^{\mathrm{T}}\mathbf{B}_0(\mathbf{V}_+-\mathbf{V}_-)\,d\Omega,$$

where $\mathbf{V}_-$ is the known solution from the last time-step.

From the point of view of finite elements, the symmetric form (2.5) is particularly interesting. An attempt to solve (2.5) with a standard Galerkin version of (2.7), i.e., without the SD-modification, would mean to seek a solution $\mathbf{V}$ such that

$$\begin{aligned}\int_{S_n}&\mathbf{w}^{\mathrm{T}}\left[\mathbf{B}_0\frac{\partial \mathbf{V}}{\partial t}+\sum_{i=1}^{d}\mathbf{B}_i\frac{\partial \mathbf{V}}{\partial x_i}\right]dS_n\\ &+\int_{\Omega}\mathbf{w}_+^{\mathrm{T}}\mathbf{B}_0(\mathbf{V}_+-\mathbf{V}_-)\,d\Omega=0.\end{aligned} \tag{2.8}$$

In the mathematical error analysis of FEM one chooses a particular test function $\mathbf{w}$ so that the variational equation yields some information concerning the properties of the

approximation, and this $\mathbf{w}$ is typically chosen equal to the solution $\mathbf{V}$. Now, for a method defined in conservation variables, such a choice does not even make dimensional sense. If, on the other hand, the system of equations is formulated in entropy variables, we have, for the continuous problem (cf. [8, 5, 11]),

$$\begin{aligned}\mathbf{v}^{\mathrm{T}}\left[\mathbf{B}_0\frac{\partial \mathbf{v}}{\partial t}+\sum_{i=1}^{d}\mathbf{B}_i\frac{\partial \mathbf{v}}{\partial x_i}\right]&=\left[\frac{\partial \eta}{\partial \mathbf{u}}\right]^{\mathrm{T}}\frac{\partial \mathbf{u}}{\partial t}+\sum_{i=1}^{d}\left[\frac{\partial \eta}{\partial \mathbf{u}}\right]^{\mathrm{T}}\mathbf{A}_i\frac{\partial \mathbf{u}}{\partial x_i}\\&=\frac{\partial \eta}{\partial t}+\sum_{i=1}^{d}\frac{\partial q_i}{\partial x_i}.\end{aligned}\tag{2.9}$$

This shows that global conservation of entropy is achieved in the Galerkin variational formulation using entropy variables, a property inherited by Galerkin FEM, which is shown by choosing $\mathbf{w}=\mathbf{V}$ in (2.8). This is an alternative explanation to why standard Galerkin FEM breaks down if the solution developes discontinuities. The role of the $\mathbf{\Theta}_E$-matrix is to ensure that the entropy inequality (2.3) holds (i.e., that the physical entropy increases) when discontinuities occur in the exact solution. In view of (2.3), the least-squares term

$$\left[\mathbf{\Theta}_E\left(\mathbf{B}_0\frac{\partial \mathbf{V}}{\partial t}+\sum_i\mathbf{B}_i\frac{\partial \mathbf{V}}{\partial x_i}\right)\right]^{\mathrm{T}}\left[\mathbf{B}_0\frac{\partial \mathbf{V}}{\partial t}+\sum_i\mathbf{B}_i\frac{\partial \mathbf{V}}{\partial x_i}\right]$$

has to be positive, which in turn means that $\mathbf{\Theta}_E$ has to be at least positive semi-definite.

The Streamline Diffusion Method in Conservation Variables

It was shown in [5] that limits of finite element solutions to conservation laws, formulated in entropy variables, converge to a weak solution and satisfy the entropy inequality. It is desirable, however, to develop a scheme which instead uses conservation variables; the relation to traditional schemes becomes clearer, and it may be simpler to establish the equations for more general gas laws (e.g., if experimental data are used). Szepessy [6] showed that the desirable theoretical properties can be retained using conservation variables, if the weighting functions $\mathbf{w}$ are chosen as $\mathbf{w}=\partial\eta/\partial\mathbf{u}$. With this choice, we obtain an entropy equality for Galerkin's method in conservation variables, using the argument (2.9). The SD-modification should then automatically yield a positive quantity, i.e., a least squares term

$$\left[\mathbf{\Theta}_E\left(\frac{\partial \mathbf{u}}{\partial t}+\sum_i\mathbf{A}_i\frac{\partial \mathbf{u}}{\partial x_i}\right)\right]^{\mathrm{T}}\left[\frac{\partial \mathbf{u}}{\partial t}+\sum_i\mathbf{A}_i\frac{\partial \mathbf{u}}{\partial x_i}\right].$$

Since

$$\mathbf{\Theta}_E\left(\frac{\partial \mathbf{u}}{\partial t}+\sum_i\mathbf{A}_i\frac{\partial \mathbf{u}}{\partial x_i}\right)=\mathbf{\Theta}_E\mathbf{B}_0\left(\mathbf{B}_0^{-1}\frac{\partial \mathbf{u}}{\partial t}+\mathbf{B}_0^{-1}\sum_i\mathbf{A}_i\frac{\partial \mathbf{u}}{\partial x_i}\right)$$

and, further, since the inverse $\mathbf{B}_0^{-1}=\partial^2\eta/\partial\mathbf{u}^2$ symmetrizes the $\mathbf{A}_i$ (since $\mathbf{B}_0^{-1}\mathbf{B}_i\mathbf{B}_0^{-1}$ must be symmetric), i.e.,

$$\mathbf{B}_0^{-1}\mathbf{A}_i=(\mathbf{B}_0^{-1}\mathbf{A}_i)^{\mathrm{T}}=\mathbf{A}_i^{\mathrm{T}}\mathbf{B}_0^{-1},$$

it follows that

$$\begin{aligned}&\mathbf{\Theta}_E\mathbf{B}_0\left(\mathbf{B}_0^{-1}\frac{\partial \mathbf{u}}{\partial t}+\sum_i\mathbf{A}_i^{\mathrm{T}}\mathbf{B}_0^{-1}\frac{\partial \mathbf{u}}{\partial x_i}\right)\\&\quad=\mathbf{\Theta}\left(\frac{\partial \mathbf{w}(\mathbf{u})}{\partial t}+\sum_i\mathbf{A}_i^{\mathrm{T}}\frac{\partial \mathbf{w}(\mathbf{u})}{\partial x_i}\right)\end{aligned}$$

with $\mathbf{\Theta}\equiv\mathbf{\Theta}_E\mathbf{B}_0$. This line of reasoning motivates the following SD-formulation: For $n=0, 1, \ldots$, find

$$\mathbf{U}=\sum_i\mathbf{U}_i\phi_i(\mathbf{x},t)\tag{2.10}$$

such that

$$\begin{aligned}&\int_{S_n}\left[\mathbf{w}+\mathbf{\Theta}\left(\frac{\partial \mathbf{w}}{\partial t}+\sum_i\mathbf{A}_i^{\mathrm{T}}\frac{\partial \mathbf{w}}{\partial x_i}\right)\right]^{\mathrm{T}}\left[\frac{\partial \mathbf{U}}{\partial t}+\sum_i\mathbf{A}_i\frac{\partial \mathbf{U}}{\partial x_i}\right]dS_n\\&\quad+\int_\Omega\mathbf{w}_+^{\mathrm{T}}(\mathbf{U}_+-\mathbf{U}_-)\,d\Omega=0\end{aligned}\tag{2.11}$$

for all $\mathbf{w}$ of the form (2.10). We note that $\partial\eta/\partial\mathbf{U}$ cannot be expressed in the form (2.10) in general, so that we instead have to work with the interpolant. The main technical difference (compared to the case of entropy variables) in the theoretical analysis is the estimation of the difference between the quantity $\partial\eta/\partial\mathbf{U}$ and its interpolant, see [6].

The convergence results in [5, 6] lean on an additional residual-based implicit artificial viscosity. In Section 4 we will introduce an explicit version of this artificial viscosity. Note, however, that the *form* of the approximation (2.11) is crucial and will be exploited in the following.

3. APPLICATION TO THE EULER EQUATIONS IN ONE DIMENSION

In this section we derive explicit expressions for the streamline perturbation matrix and discuss explicit one-step methods. Furthermore, we show the relation to traditional finite difference schemes.

Derivation of the Streamline Diffusion Matrix

In the Euler equations, the conservation variables and flux vector are given by

$$\mathbf{u}=\begin{bmatrix}\varrho\\ \varrho u\\ \varrho e\end{bmatrix}$$

$$\mathbf{f}=\begin{bmatrix}\varrho u\\ \varrho u^2+p\\ u(\varrho e+p)\end{bmatrix},$$

where $p=\varrho(\gamma-1)(e-\frac{1}{2}u^2)$. The Jacobian matrix $\mathbf{A}=\mathbf{f}'(\mathbf{u})$ is given by

$$\mathbf{A}=\begin{bmatrix}0 & 1 & 0\\ \frac{1}{2}(\gamma-3)u^2 & (3-\gamma)u & \gamma-1\\ (\gamma-1)u^3-\gamma ue & \gamma e-3(\gamma-1)u^2/2 & \gamma u\end{bmatrix}, \tag{3.1}$$

with eigenvalues $\lambda_1=u-c$, $\lambda_2=u$, and $\lambda_3=u+c$, where $c=(\gamma p/\varrho)^{1/2}$ is the sound speed. It is possible to construct a matrix $\mathbf{S}$ such that

$$\mathbf{S}^{-1}\mathbf{A}\mathbf{S}=\mathbf{\Lambda},$$

where $\mathbf{\Lambda}=\operatorname{diag}(\lambda_1,\lambda_2,\lambda_3)$ is a diagonal matrix containing the eigenvalue of $\mathbf{A}$. The matrices $\mathbf{S}$ and $\mathbf{S}^{-1}$ are given by

$$\mathbf{S}=\begin{bmatrix}1 & 1 & 1\\ u-c & u & u+c\\ H-uc & u^2/2 & H+uc\end{bmatrix}$$

and

$$\mathbf{S}^{-1}=\frac{1}{2Hc-u^2c}\times\begin{bmatrix}u(uc-u^2+2H)/2 & u^2/2-uc-H & c\\ 2(Hc-u^2c) & 2uc & -2c\\ u(uc+u^2-2H)/2 & -u^2/2-uc+H & c\end{bmatrix},$$

where $H=e+p/\varrho$ is the enthalpy.

In order to determine explicit expressions for the $\mathbf{\Theta}$-matrix in the case of systems of conservation laws, it is instructive first to consider the constant coefficient case

$$\frac{\partial\mathbf{u}}{\partial t}+\mathbf{A}\frac{\partial\mathbf{u}}{\partial x}=0, \tag{3.2}$$

with $\mathbf{A}$ a constant matrix, diagonalizable as above. The SD-method for (3.2) can be written

$$\int_{S_n}\left[\mathbf{w}+\mathbf{\Theta}\left(\frac{\partial\mathbf{w}}{\partial t}+\mathbf{A}^{\mathrm{T}}\frac{\partial\mathbf{w}}{\partial x}\right)\right]^{\mathrm{T}}\left[\frac{\partial\mathbf{U}}{\partial t}+\mathbf{A}\frac{\partial\mathbf{U}}{\partial x}\right]dS_n$$
$$+\int_{\Omega}\mathbf{w}_+^{\mathrm{T}}(\mathbf{U}_+-\mathbf{U}_-)\,d\Omega=0. \tag{3.3}$$

Following [1], we introduce new variables $\bar{\mathbf{U}}=\mathbf{S}^{-1}\mathbf{U}$ and $\bar{\mathbf{w}}=\mathbf{S}^{\mathrm{T}}\mathbf{w}$ to obtain

$$\left[\mathbf{S}^{-\mathrm{T}}\bar{\mathbf{w}}+\mathbf{\Theta}\left(\mathbf{S}^{-\mathrm{T}}\frac{\partial\bar{\mathbf{w}}}{\partial t}+\mathbf{A}^{\mathrm{T}}\mathbf{S}^{-\mathrm{T}}\frac{\partial\bar{\mathbf{w}}}{\partial x}\right)\right]^{\mathrm{T}}\left[\mathbf{S}\frac{\partial\bar{\mathbf{U}}}{\partial t}+\mathbf{A}\mathbf{S}\frac{\partial\bar{\mathbf{U}}}{\partial x}\right]$$
$$=\left[\bar{\mathbf{w}}+\mathbf{S}^{\mathrm{T}}\mathbf{\Theta}\mathbf{S}^{-\mathrm{T}}\left(\frac{\partial\bar{\mathbf{w}}}{\partial t}+\mathbf{\Lambda}\frac{\partial\bar{\mathbf{w}}}{\partial x}\right)\right]^{\mathrm{T}}\left[\frac{\partial\bar{\mathbf{U}}}{\partial t}+\mathbf{\Lambda}\frac{\partial\bar{\mathbf{U}}}{\partial x}\right]. \tag{3.4}$$

The last expression is a set of uncoupled equations. For each component, we now know the amount of SD-perturbation to be added. We obtain

$$\mathbf{S}^{\mathrm{T}}\mathbf{\Theta}\mathbf{S}^{-\mathrm{T}}=(\delta_k\mathbf{I}+\delta_h\mathbf{\Lambda}^2)^{-1/2}, \tag{3.5}$$

where $\delta_k=4/k_n^2$ and $\delta_h=4/h^2$, k_n denotes the timestep and h denotes the local meshsize, see, e.g., [3]. Thus

$$\mathbf{\Theta}=[\mathbf{S}(\delta_k\mathbf{I}+\delta_h\mathbf{\Lambda}^2)^{-1/2}\mathbf{S}^{-1}]^{\mathrm{T}}=[(\delta_k\mathbf{I}+\delta_h\mathbf{A}^2)^{-1/2}]^{\mathrm{T}}. \tag{3.6}$$

This derivation is certainly not valid in case $\mathbf{A}$ is non-linear, in which case we must consider a linearization (somewhat ad hoc, since $\mathbf{U}$ is continuous be definition). In the following we shall see, however, that the choice (3.6) is closely related to traditional schemes.

Explicit Formulation and the Relation to Finite Difference Schemes

The simplest possible scheme consists of a linear approximation in space and a piecewise constant approximation in time, which yields

$$\int_{S_n}\left(\mathbf{w}^{\mathrm{T}}\frac{\partial\mathbf{f}}{\partial x}+\left(\frac{\partial\mathbf{w}}{\partial x}\right)^{\mathrm{T}}\mathbf{A}\mathbf{\Theta}^{\mathrm{T}}\mathbf{A}\frac{\partial\mathbf{U}}{\partial x}\right)dS_n$$
$$+\int_{\Omega}\mathbf{w}_+^{\mathrm{T}}(\mathbf{U}_+-\mathbf{U}_-)\,d\Omega=0. \tag{3.7}$$

In order to obtain a genuinely explicit scheme, the solution is "frozen" at time $t=t_n$. Furthermore, the mass matrix resulting from the jump term is lumped, which in this case corresponds to the use of nodal quadrature. The quadrature error is of order $O(h^2)$ for linear elements, so mass lumping

will have no effect on the accuracy of the scheme (although it is well known that mass lumping has a viscous effect).

With these simplifications, we obtain the following scheme, setting $\mathbf{U}^{n+1} \equiv \mathbf{U}_+$, $\mathbf{U}^n \equiv \mathbf{U}_-$, and $\mathbf{f}^n \equiv \mathbf{f}(\mathbf{U}^n)$:

$$\mathbf{U}_i^{n+1} = \mathbf{U}_i^n - \frac{k_n}{h} \int_{x_{i-1}}^{x_{i+1}} \left(\frac{\partial \mathbf{w}}{\partial x}\right)^{\mathrm{T}} \times \left(-\mathbf{f}^n + \mathbf{A}\boldsymbol{\Theta}^{\mathrm{T}}\mathbf{A} \frac{\partial \mathbf{U}^n}{\partial x} \right) dx. \tag{3.8}$$

In order to compare the SD-method with traditional finite difference schemes, we make a simplification in the choice of $\boldsymbol{\Theta}$. With a constant temporal approximation on each space-time slab the term $\partial \mathbf{U}/\partial t$ equals zero within the slab, and it is then natural to drop the identity matrix in (3.6) (which is motivated by the control of the temporal derivatives in the residual). On a fixed, equally spaced mesh, and with the specific ("optimal," cf. [2]) choice

$$\boldsymbol{\Theta}^{\mathrm{T}} = \tfrac{1}{2} h (\mathbf{A}^2)^{-1/2} = \tfrac{1}{2} h \, |\mathbf{A}|^{-1},$$

the scheme becomes

$$\mathbf{U}_i^{n+1} = \mathbf{U}_i^n - \frac{k_n}{h} \int_{x_{i-1}}^{x_{i+1}} \left(\frac{\partial \mathbf{w}}{\partial x}\right)^{\mathrm{T}} \times \left(-\mathbf{f}^n + \frac{1}{2} h \, |\mathbf{A}(\mathbf{U}^n)| \frac{\partial \mathbf{U}^n}{\partial x} \right) dx. \tag{3.9}$$

With a linear spatial approximation, the components of $\partial \mathbf{w}/\partial x$ (i.e., $\partial \phi_i/\partial x$) equal h^{-1} left of node i and $-h^{-1}$ right of node i, so that

$$-\int_{x_{i-1}}^{x_{i+1}} \left(\frac{\partial \mathbf{w}}{\partial x}\right)^{\mathrm{T}} \mathbf{f}^n \, dx = \frac{1}{h} \left(\int_{x_i}^{x_{i+1}} \mathbf{f}^n \, dx - \int_{x_{i-1}}^{x_i} \mathbf{f}^n \, dx \right).$$

If these integrals are evaluated using endpoint averages, we obtain the finite difference approximation $\frac{1}{2}(\mathbf{f}_{i+1}^n - \mathbf{f}_{i-1}^n)$. It is then clear that the scheme (3.9) is a FEM-generalization of upstream-type difference schemes, depending on the integration rule for the term

$$\int_{x_{i-1}}^{x_i} |\mathbf{A}(\mathbf{U}^n)| \frac{\partial \mathbf{U}^n}{\partial x} \, dx,$$

viz.,

- Van Leer [12], $\frac{1}{2}(|\mathbf{A}_{i-1}| + |\mathbf{A}_i|)(\mathbf{U}_i^n - \mathbf{U}_{i-1}^n)$
- Osher and Solomon [13], $\int_\Gamma |\mathbf{A}(\mathbf{U})| \, d\mathbf{U}$, where Γ joins $\mathbf{U}_{i-1}^n$ and $\mathbf{U}_i^n$
- Steger and Warming [14], $|\mathbf{A}_i| \, \mathbf{U}_i^n - |\mathbf{A}_{i-1}| \, \mathbf{U}_{i-1}^n$
- Vijayasundaram [15], $|\mathbf{A}_{i-1/2}| \, (\mathbf{U}_i^n - \mathbf{U}_{i-1}^n)$.

Here, $\mathbf{A}_i \equiv \mathbf{A}(\mathbf{U}_i^n)$ and $\mathbf{A}_{i-1/2} \equiv \mathbf{A}(\frac{1}{2}(\mathbf{U}_i^n + \mathbf{U}_{i-1}^n))$. Note, however, that the path Γ in the Osher–Solomon scheme does not coincide with the straight line joining $\mathbf{U}_{n-1}$ and $\mathbf{U}_n$ as in (3.9) and that Vijayasundaram uses an alternative integration rule for the flux (his scheme in fact corresponds to one-point Gaussian integration in (3.9)).

If, on the other hand, the SD-matrix $\boldsymbol{\Theta}$ is chosen as

$$\boldsymbol{\Theta}^{\mathrm{T}} = \tfrac{1}{2} k_n \mathbf{I}$$

then, as noted in [1], we obtain a variant of the Lax–Wendroff (or Taylor–Galerkin [16]) method, the crucial point now being the evaluation of $\int_{x_{i-1}}^{x_i} [\mathbf{A}(\mathbf{U}^n) \, \partial \mathbf{f}^n/\partial x] \, dx$. To compare with finite differences we may write, e.g.,

$$\int_{x_{i-1}}^{x_i} \mathbf{A}(\mathbf{U}^n) \frac{\partial \mathbf{f}^n}{\partial x} \, dx \simeq \mathbf{A}_{i-1/2}(\mathbf{f}_i^n - \mathbf{f}_{i-1}^n).$$

Thus, in finite difference terminology, the SD-method may be seen as a combination of the upstream and Lax–Wendroff methods, but both methods fit in the general framework (indeed, if we were to set $\boldsymbol{\Theta}^{\mathrm{T}} = (\vartheta \, \delta_k \mathbf{I} + (1-\vartheta) \, \delta_h \mathbf{A}^2)^{-1/2}$, we would see a continuous transfer from the highly dispersive behaviour of Lax–Wendroff type schemes, at $\vartheta = 1$, to the monotone upwind behaviour at $\vartheta = 0$).

The subject of upstream- and Godunov-type methods has been reviewed by Harten *et al.* [17].

4. APPLICATION TO THE TWO-DIMENSIONAL EULER EQUATIONS

This section deals with the extension of the preceding approach to the multi-dimensional setting. An explicit artificial viscosity, based on the FEM-residual, is introduced to avoid under- or overshoot. For simplicity, we will restrict the exposition to finite elements that are equally spaced in different directions in space, i.e., without stretching. The problem of how to treat stretched elements has been considered by Hughes and Mallet [2].

General Problems Facing Multi-dimensional Schemes

Assume that we are given a linear convective system of the form

$$\frac{\partial \mathbf{u}}{\partial t} + \sum_i \mathbf{A}_i \frac{\partial \mathbf{u}}{\partial x_i} = 0, \tag{4.1}$$

and that all of the matrices $\mathbf{A}_i$ are simultaneously diagonalizable using the same similarity transformation, i.e.,

$$\mathbf{S}^{-1}\mathbf{A}_i\mathbf{S} = \boldsymbol{\Lambda}_i. \tag{4.2}$$

Reasoning as above, we obtain a diagonal system for the formulation (2.11), and the SD-perturbation becomes, in analogue with (3.6),

$$\Theta = \left[\left(\delta_k \mathbf{I} + \delta_h \sum_i \mathbf{A}_i^2\right)^{-1/2}\right]^{\mathrm{T}}. \tag{4.3}$$

In general it is not possible to simultaneously diagonalize an advective system, and in particular this is the case for the Jacobian matrices in the quasi-linear formulation of the multi-dimensional Euler equations. This crucial fact may lead us to choose an alternative route, e.g., selecting a specified direction in which to introduce streamline diffusion. It is well known, however, that, for the Euler equations, the individual matrices $\mathbf{A}_i$ are simultaneously *symmetrized* by the same similarity transformation (see [18]). Indeed, such a symmetrization follows from the existence of entropy variables. For it follows from the symmetry of the matrices

$$\mathbf{B}_i = \mathbf{A}_i \mathbf{B}_0$$

and

$$(\mathbf{B}_0)^{-1/2}\, \mathbf{B}_i (\mathbf{B}_0)^{-1/2} = (\mathbf{B}_0)^{-1/2}\, \mathbf{A}_i (\mathbf{B}_0)^{1/2}$$

(cf. Harten [10]) that a similarity transformation like (4.2), with $\mathbf{S} = (\mathbf{B}_0)^{1/2}$, will yield a symmetric, positive semi-definite matrix for all i. This means that the matrix $\mathbf{C} = \delta_k \mathbf{I} + \delta_h \sum_i \mathbf{A}_i^2$ is similar to a symmetric positive-definite matrix and thus has real positive eigenvalues and a complete set of eigenvectors. Consequently, $\mathbf{C}$ has a computable inverse square root and (4.3) is well defined.

We are thus led to the following possibilities regarding the choice of Θ in a multi-dimensional problem:

(i) To choose a particular upwind direction (cf. Davis [19]).

(ii) To use (4.3) as a definition of Θ, cf. [2].

We consider these approaches separately in the following sections. In analogy with (3.9), we will consider constant-in-time approximations only, and set $\delta_k = 0$; the latter choice clarifies the relation to existing schemes.

Directionally Biased Streamline Diffusion Matrices

Assume that the solution to the two-dimensional Euler equations is dominated by a single discontinuity, occurring in all of the variables u_j, the contour of which has a unit normal vector $\mathbf{n} = (n_1, n_2)$ in the (x_1, x_2)-plane. We then have a quasi one-dimensional problem which may be written

$$\frac{\partial \mathbf{u}}{\partial t} + (\mathbf{A}_1 n_1 + \mathbf{A}_2 n_2) \frac{\partial \mathbf{u}}{\partial n} = 0. \tag{4.4}$$

Since the matrix

$$\mathbf{A}_n = \mathbf{A}_1 n_1 + \mathbf{A}_2 n_2$$

possesses real eigenvalues and a complete set of eigenvectors, given in the Appendix, we may return to the one-dimensional formulation to obtain the following two-dimensional analogue to (3.9):

$$\mathbf{U}_i^{n+1} = \mathbf{U}_i^n - \frac{k}{m(\Omega_L)} \int_{\Omega_E} \sum_i \left[-\left(\frac{\partial \mathbf{w}}{\partial x_i}\right)^{\mathrm{T}} \mathbf{f}_i^n \right] + \frac{h}{2} \left(\frac{\partial \mathbf{w}}{\partial n}\right)^{\mathrm{T}} |\mathbf{A}_n(\mathbf{U}^n)| \frac{\partial \mathbf{U}^n}{\partial n}\, d\mathbf{x}. \tag{4.5}$$

Here Ω_E denotes the domain covered by the elements sharing node i, and $m(\Omega_L)$ denotes the area of Ω_L, the domain of influence obtained when lumping the consistent mass matrix in two dimensions (a "median element"), see Fig. 1.

We may rewrite Equation (4.5), using the identity $\partial/\partial n \equiv n_1\, \partial/\partial x_1 + n_2\, \partial/\partial x_2$, to obtain

$$\mathbf{U}_i^{n+1} = \mathbf{U}_i^n - \frac{k}{m(\Omega_L)} \int_{\Omega_E} \left(\sum_i \left[-\left(\frac{\partial \mathbf{w}}{\partial x_i}\right)^{\mathrm{T}} \mathbf{f}_i^n \right] + \frac{h}{2} (\nabla \mathbf{w})^{\mathrm{T}} \mathbf{C}_n \nabla \mathbf{U}^n \right) d\mathbf{x}, \tag{4.6}$$

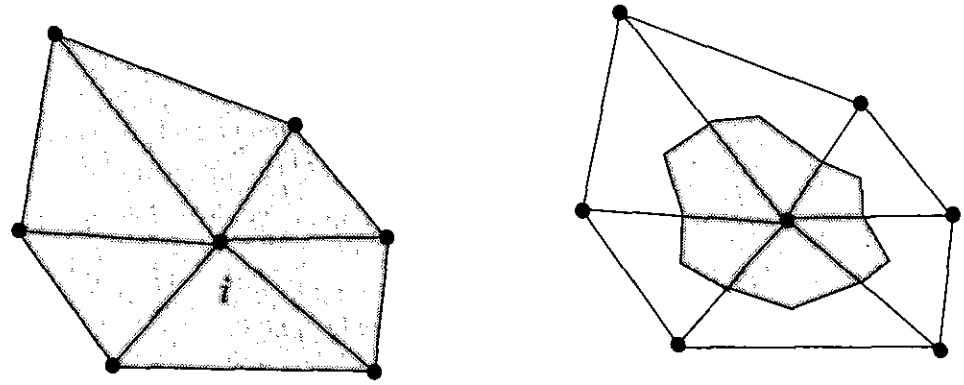

FIG. 1. The domains Ω_E and Ω_L.

where

$$\nabla \mathbf{w} = \left(\frac{\partial w_1}{\partial x_1}, \ldots, \frac{\partial w_4}{\partial x_1}, \frac{\partial w_1}{\partial x_2}, \ldots, \frac{\partial w_4}{\partial x_2} \right)^{\mathrm{T}}$$

and

$$\mathbf{C}_n = \begin{bmatrix} n_1^2 |\mathbf{A}_n| & n_1 n_2 |\mathbf{A}_n| \\ n_1 n_2 |\mathbf{A}_n| & n_2^2 |\mathbf{A}_n| \end{bmatrix}. \tag{4.7}$$

$\mathbf{C}_n$ thus plays the role of a regularizing viscosity matrix. The scheme (4.6) then ideally corresponds to using central differencing tangentially to a shock and upstream differencing across it, an approach closely related to that of Davis [19].

It is worth noting that in (Godunov-type) finite difference- and finite volume methods this type of single discontinuity is *enforced* by *defining* the solution to be piecewise constant, linear, etc. Typically, in finite differences, one considers one-dimensional Riemann solvers applied to the x_1- and x_2-directions alternately; this approach may be mimicked in the present context by choosing

$$\mathbf{C}_n^* = \begin{bmatrix} \frac{1}{2} |\mathbf{A}_1| & \mathbf{0} \\ \mathbf{0} & \frac{1}{2} |\mathbf{A}_2| \end{bmatrix}. \tag{4.8}$$

In finite volume methods (or rather, FEM with a piecewise continuous approximation), the discontinuities occur at the boundaries of the "cells" whether they consist of domains such as Ω_L, cf. [15, 20], or triangles, cf. [21, 22].

The concept of directional biasing thus shows the relation to traditional schemes also in a multi-dimensional setting, the crucial difference being that the SD-method yields a possibility to do upwinding *consistently* in the sense that a weak formulation of the type (2.11) exists.

A Streamline Diffusion Matrix Based on Approximate Diagonalization

The concept of directional biasing is consistent with the weak formulation (2.11) only if the discontinuities have a restricted appearance, so that the multi-dimensional problem may be reduced to a one-dimensional analogue. A natural *consistent* way of choosing the SD-matrix $\mathbf{\Theta}$ is given by (4.3). The analogue to this choice, in the case of entropy variables (and thus *symmetric* Jacobian matrices), was first advocated by Hughes and Mallet [2], who pointed out that it satisfies a number of desirable design conditions, viz.,

(i) It reduces to the standard SD-formulation for one-dimensional convective systems.

(ii) It coincides with the standard SD-formulation for scalar multidimensional convection problems.

(iii) For simultaneously diagonalizable convective systems, it coincides with the standard SD-formulation with respect to each uncoupled scalar equation.

Thus, for the Euler equations in two dimensions, the matrix

$$\mathbf{\Theta}^{\mathrm{T}} = \frac{h}{2} \left(\sum_{i=1}^{2} \mathbf{A}_i^2 \right)^{-1/2}$$

is of special interest. To be able to compute it, we need the eigenvalues and eigenvectors of $\mathbf{C} = \sum_{i=1}^{2} \mathbf{A}_i^2$, which are given in the Appendix. The analogue to (4.6) may then be written

$$\mathbf{U}_i^{n+1} = \mathbf{U}_i^n - \frac{k}{m(\Omega_L)} \int_{\Omega_E} \left(\sum_i \left[-\left(\frac{\partial \mathbf{w}}{\partial x_i} \right)^{\mathrm{T}} \mathbf{f}_i^n \right] + \frac{h}{2} \nabla \mathbf{w}^{\mathrm{T}} \mathbf{C}_A \nabla \mathbf{U}^n \right) d\mathbf{x}, \tag{4.9}$$

with viscosity matrix

$$\mathbf{C}_A = \begin{bmatrix} \mathbf{A}_1 \mathbf{\Theta}^{\mathrm{T}} \mathbf{A}_1 & \mathbf{A}_1 \mathbf{\Theta}^{\mathrm{T}} \mathbf{A}_2 \\ \mathbf{A}_2 \mathbf{\Theta}^{\mathrm{T}} \mathbf{A}_1 & \mathbf{A}_2 \mathbf{\Theta}^{\mathrm{T}} \mathbf{A}_2 \end{bmatrix}. \tag{4.10}$$

Note that directional biasing and approximate diagonalization may coincide in case the Jacobians are simultaneously diagonalizable, since then the components of $\mathbf{C}_A$ will satisfy

$$\mathbf{A}_i \mathbf{\Theta}^{\mathrm{T}} \mathbf{A}_j = \mathbf{S} \mathbf{\Lambda}_A \mathbf{S}^{-1},$$

where

$$\mathbf{\Lambda}_A = \operatorname{diag} \left(\frac{\lambda_{i,1} \lambda_{j,1}}{(\sum_k \lambda_{k,1}^2)^{1/2}}, \frac{\lambda_{i,2} \lambda_{j,2}}{(\sum_k \lambda_{k,2}^2)^{1/2}}, \ldots \right),$$

and the $\lambda_{i,j}$ are the j components of the $\mathbf{\Lambda}_i$ in (4.2). The components of $\mathbf{C}_n$ will satisfy

$$n_i n_j |\mathbf{A}_n| = \mathbf{S} \mathbf{\Lambda}_n \mathbf{S}^{-1},$$

where

$$\mathbf{\Lambda}_n = \operatorname{diag} \left(n_i n_j \left| \sum_k n_k \lambda_{k,1} \right|, n_i n_j \left| \sum_k n_k \lambda_{k,2} \right|, \ldots \right).$$

The two matrices $\mathbf{\Lambda}_A$ and $\mathbf{\Lambda}_n$ will coincide if, for each diagonal element,

$$n_i = \frac{\lambda_{i,j}}{(\sum_k \lambda_{k,j}^2)^{1/2}},$$

which corresponds to upwinding in the generalized streamline direction. In order to be able to choose a distinct direction $\mathbf{n}$, all information must travel in the same direction which is not the case in general.

A Non-linear Artificial Viscosity Term

Depending on the choice of SD-matrix, we may obtain monotonous solutions or solutions displaying spurious oscillations close to discontinuities in the flowfield (note, for instance, the Lax–Wendroff choice, discussed in the one-dimensional context, with well-known dispersive qualities). To stabilize the solution, we utilize the fact that we have a solution defined *everywhere* in the domain. This solution does not necessarily fulfill the differential equation, i.e.,

$$\mathbf{R}(\mathbf{U}) \equiv \frac{\partial \mathbf{U}}{\partial t} + \sum_i \frac{\partial \mathbf{f}_i(\mathbf{U})}{\partial x_i} \neq 0,$$

in general. The size of the residual, $|\mathbf{R}|$, will be (very) small away from discontinuities and large (typically $O(h^{-1})$) close to a shock, see [7] for a further discussion. These qualities qualify $\mathbf{R}$ as a base for constructing an automatic artificial viscosity which adds $O(h)$-viscosity close to discontinuities and vanishes in smooth regions. We have implemented an explicit version of such an artificial viscosity, with the following appearance: add to the original scheme, e.g., Eq. (4.9), a term on the right-hand side,

$$-\frac{k}{m(\Omega_L)} \int_{\Omega_E} \delta_v (\nabla \mathbf{w})^{\mathrm{T}} \nabla \mathbf{U}^n \, d\mathbf{x}.$$

Here,

$$\delta_v \simeq h \frac{|\mathbf{R}(\mathbf{U}^{n-1})|}{|\nabla \mathbf{U}^{n-1}| + \varepsilon}, \tag{4.11}$$

with $\mathbf{R}(\mathbf{U}^{n-1})$ approximated by

$$\mathbf{R}(\mathbf{U}^{n-1}) \approx \frac{\mathbf{U}^{n-1} - \mathbf{U}^{n-2}}{k_{n-1}} + \sum_i \mathbf{A}_i(\mathbf{U}^{n-1}) \frac{\partial \mathbf{U}^{n-1}}{\partial x_i}.$$

(To avoid confusing dimensions, the $\mathbf{U}$ occurring in (4.11) should be made non-dimensional.) The gradient of $\mathbf{U}$ is included to normalize the artificial viscosity, and ε is a small positive number included in order to avoid division by zero (we have used $\varepsilon = h$).

Order of Convergence

The SD-methods presented here are, viewed as time-accurate schemes, at most first-order accurate since we use a piecewise constant temporal approximation. An important feature of the *consistent* SD-methods, e.g., (4.9), is that they are "second-order" accurate *in space* (or, more precisely, the root-mean-square error is of the order $O(h^{3/2})$). This leads us to expect that stationary shocks will be well resolved. The higher order accuracy is closely related to the consistency of the SD-method (in that the discrete equation is fulfilled weakly in the sense of (2.11)); it does not just consist of adding a first-order artificial viscosity, which would yield first-order accuracy in both space and time.

In the numerical examples of the following section, we shall see that the consistent SD-method, following from the choice (4.10), indeed yields a better resolution of stationary shocks as compared with the inconsistent but related choice (4.8).

If we desire higher order accuracy also in time, in the usual framework of SD-methods, a linear temporal approximation should be used. This choice is more natural to use in an implicit scheme. In Section 3 we noted, however, that the order may also hinge on the selection of Θ; we may, e.g., obtain higher order schemes of Lax–Wendroff type.

5. NUMERICAL EXAMPLES

In this section we show the effect of some different choices of SD-matrices in two dimensions. In particular, we point out the small amount of numerical diffusion obtained with approximate diagonalization. The diagonal biasing effect has been introduced by setting $\mathbf{n} = \nabla p$ (i.e., the gradient of the pressure from the preceding timestep) in (4.5).

Sod's Problem in Two Dimensions

This one-dimensional Riemann problem due to Sod [23] has been extended to two dimensions by considering one row of 100 square elements with the vertical velocity prescribed to zero. The results are shown after 50 timesteps with $k/h = 0.411$. Sod's problem is that of a shock tube in which a membrane separtates two different states of a per-

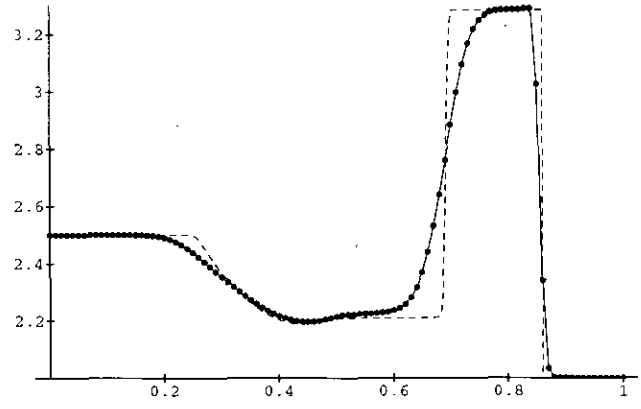

FIG. 2. Directionally biased SD-matrix.

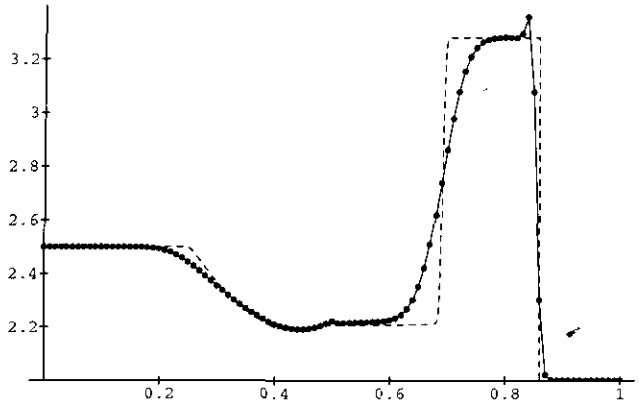

FIG. 3. Approximately diagonalized SD-matrix.

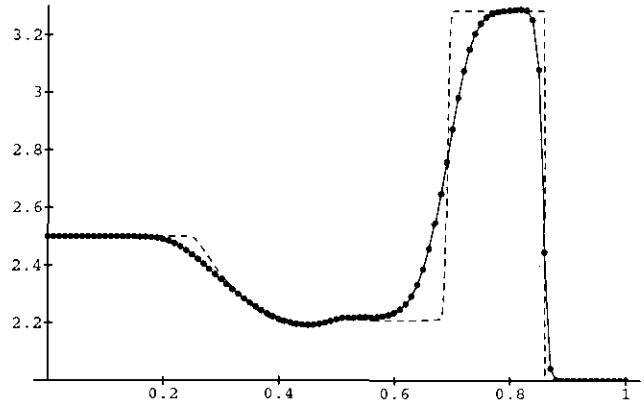

FIG. 4. Approximately diagonalized SD-matrix with artificial viscosity.

fect gas. The initial data are given by $\rho = 1$, $u = 0$, $p = 1$ if $x_1 \leqslant \frac{1}{2}$, and $\rho = 0.125$, $u = 0$, $p = 0.1$ if $x_1 > \frac{1}{2}$; $\gamma = 1.4$. The computational domain is $0 \leqslant x_1 \leqslant 1$, $0 \leqslant x_2 \leqslant 0.01$. The membrane is removed instantaneously at $t = 0$. We show here only the internal energy, the features of which are, from left to right, a rarefaction wave (moving into the high-pressure gas), followed by a contact discontinuity and a shock (both moving into the low-pressure gas, but with different speeds). The shock is typically easiest to resolve (due to overtaking characteristics), whereas the contact discontinuity and rarefaction wave will be more or less smeared, depending on the order of the scheme.

Figure 2 shows the internal energy using the directionally biased method, which in this case coincides with the one-dimensional version. Evidently, the method yields a reasonably good first-order scheme for one-dimensional problems.

Figure 3 shows the internal energy using approximate diagonalization. Note the slight oscillations, which are removed when we apply the residual-based artificial viscosity (Fig. 4).

Shock Reflection

This example of stationary shock reflection was employed by Davis [19] as a test of shock spreading. The domain is four units long and one unit high. We have used initial and inflow boundary conditions on the left-hand side of the domain given by $\mathbf{U} = (1.0, 2.9, 0, 5.99)^T$, and the inflow condition at the top of the domain was set to $\mathbf{U} = (1.7, 4.45, 0.86, 9.87)^T$. At the bottom of the domain, the normal velocity was prescribed to zero. The exact solution to this problem is given by an incident shock at a 29° angle to the top of the domain, which is reflected at the bottom of the domain and exits just below the top on the right-hand side of the domain.

The problem has been solved both with square bilinear elements and with linear triangular elements. In the case of triangular elements, we used an adaptive scheme described in [7]. In particular, we use an adaptive mesh generator based on an underlying quadrilateral grid. The quadrilaterals are divided into two (or, for transition elements, more) triangles, and the diagonal may be flipped adaptively to align with a direction perpendicular to the gradient of the solution. This simple additional adaptive feature may give substantially improved results, see [4].

The converged pressure is shown in Figs. 5–8 for square elements, and in Figs. 9–11 for triangular elements. (Because of lack of software, the carpet plots utilise triangular elements.) In Fig. 9, we have mimicked the traditional piecewise constant finite volume/FEM-schemes by choosing three Gauss points on the edges of the triangles. In each Gauss point we assume that there is a discontinuity aligned with the element side so that we may use $\mathbf{A}_n$ locally,

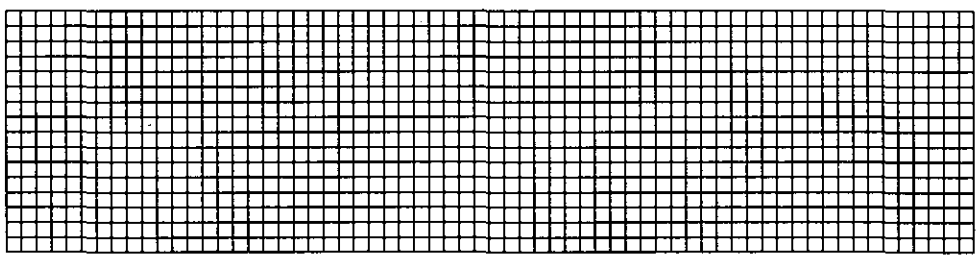

FIG. 5. Mesh for the computation with bilinear elements.

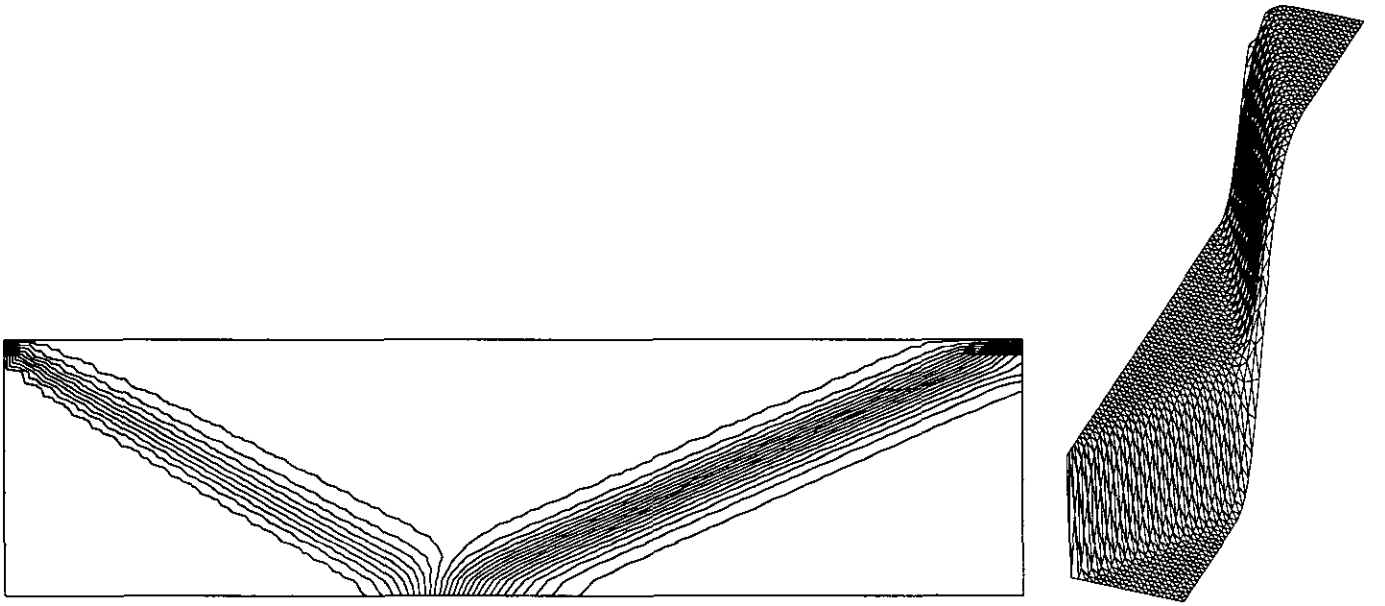

FIG. 6. Viscosity matrix C_n^*, square elements.

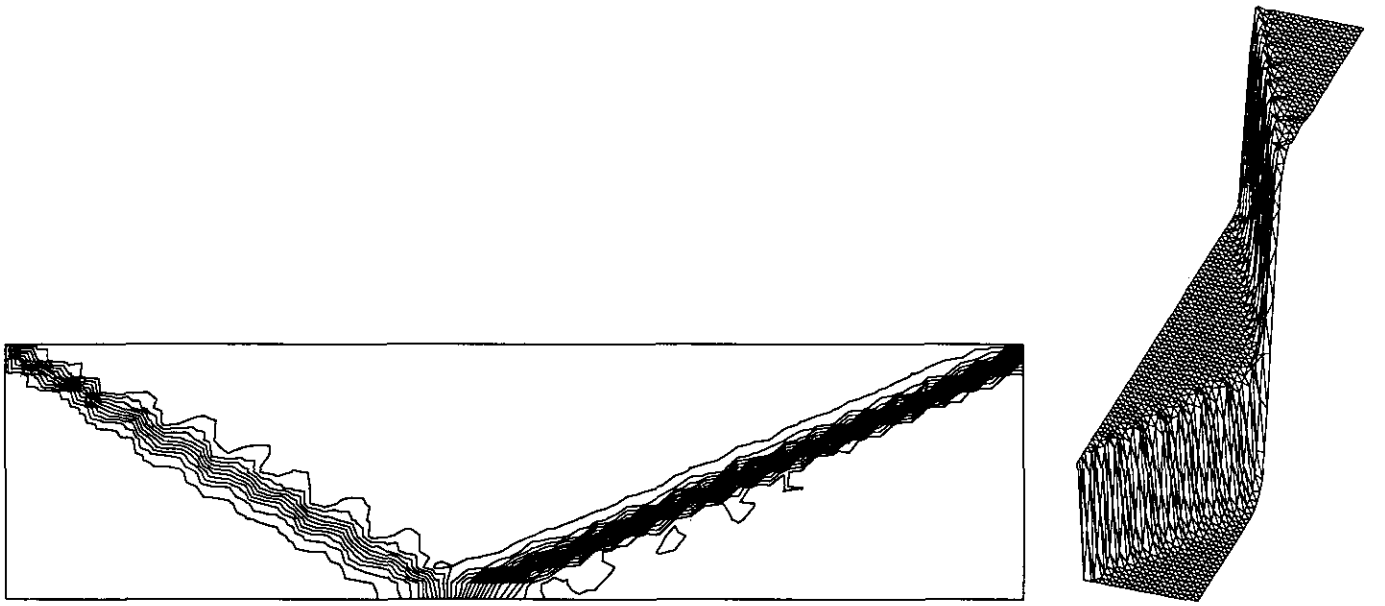

FIG. 7. Viscosity matrix C_n, square elements.

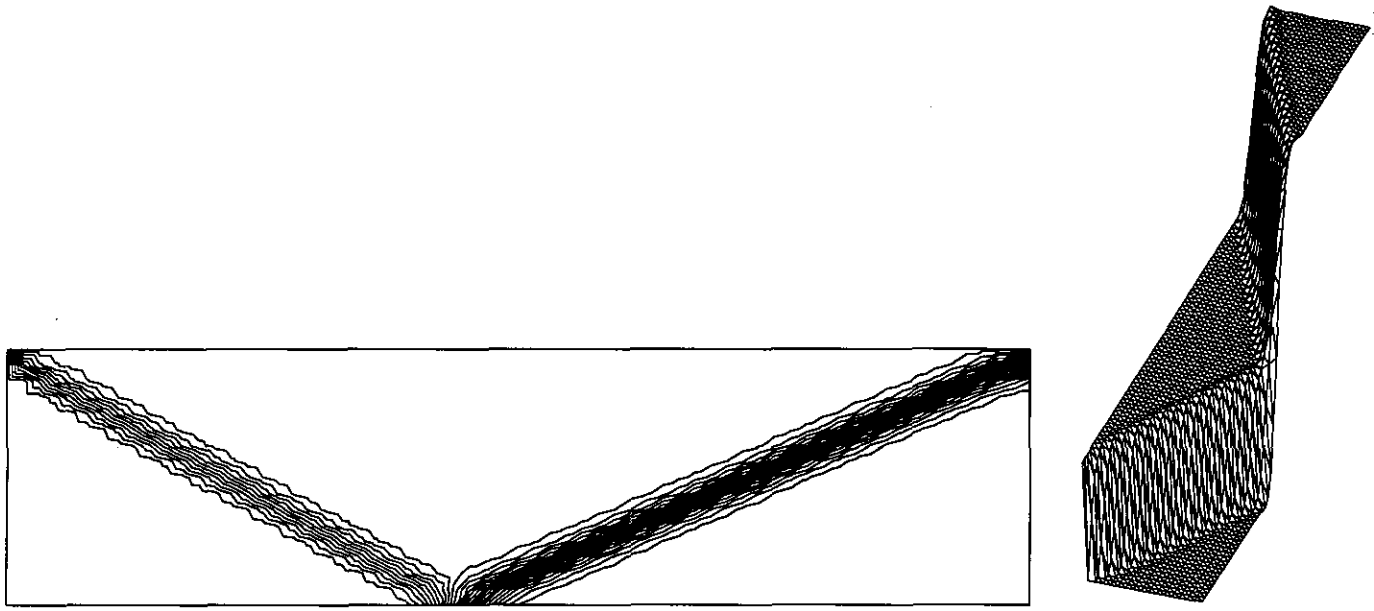

FIG. 8. Viscosity matrix C_A, square elements.

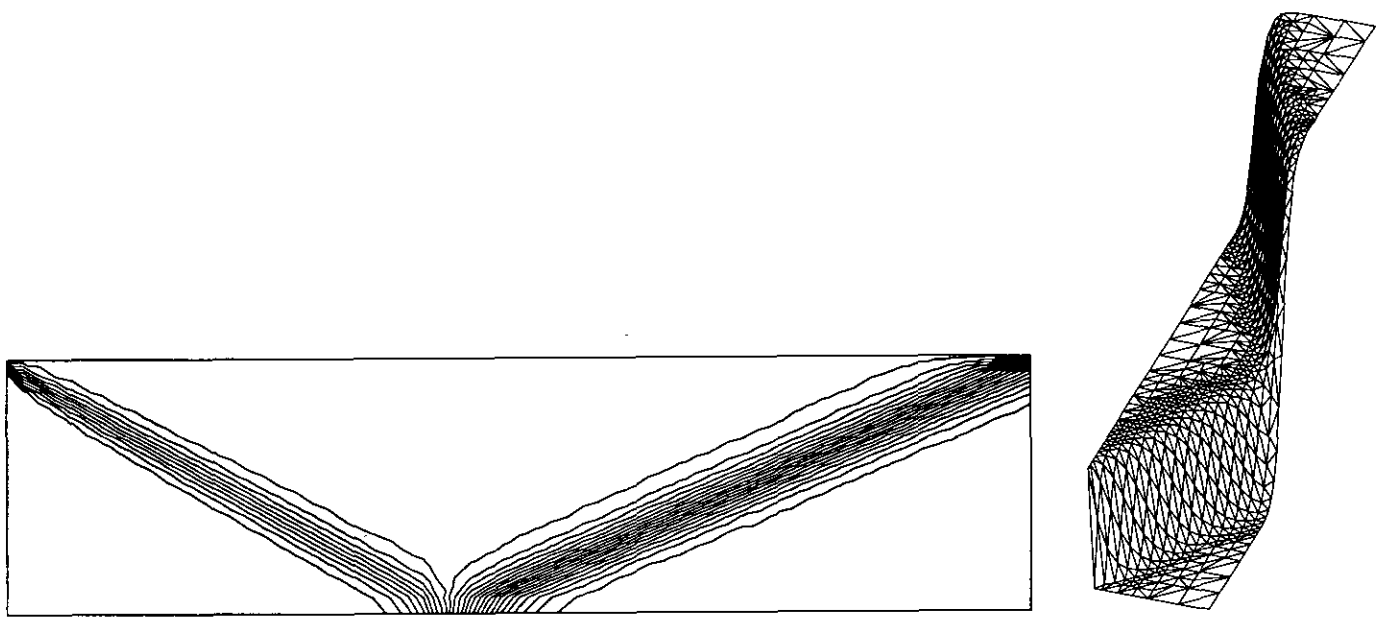

FIG. 9. Viscosity matrix mimicking piecewise constants, triangular elements.

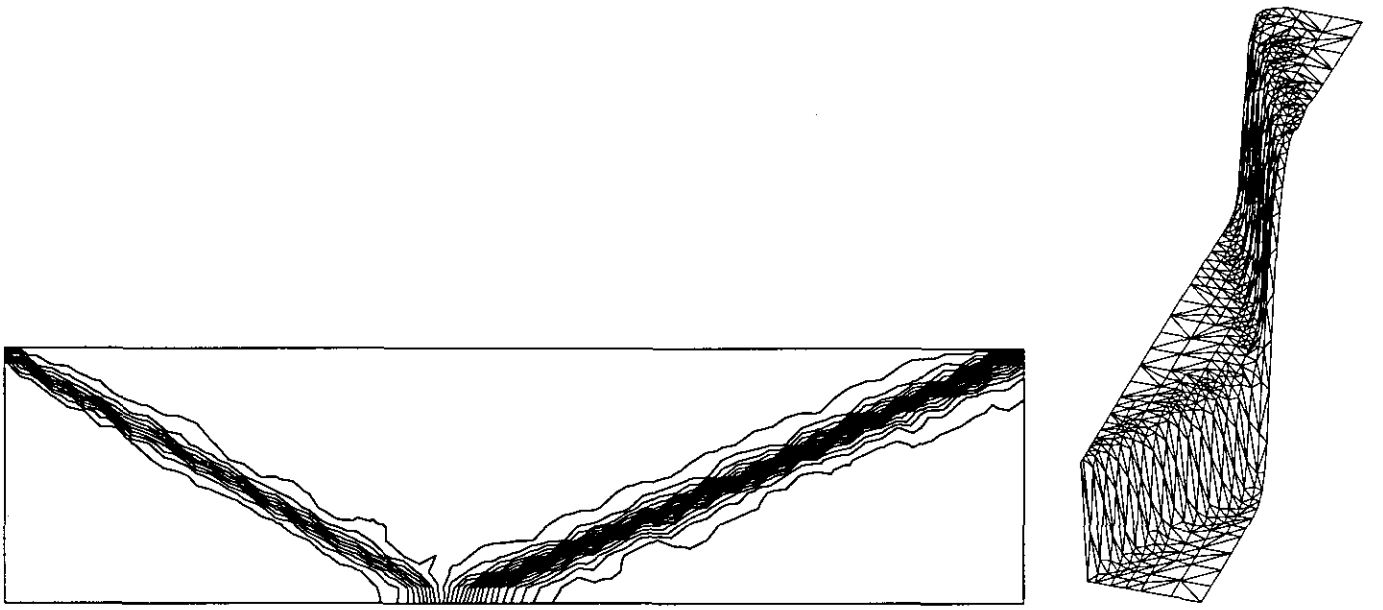

FIG. 10. Viscosity matrix C_n, triangular elements.

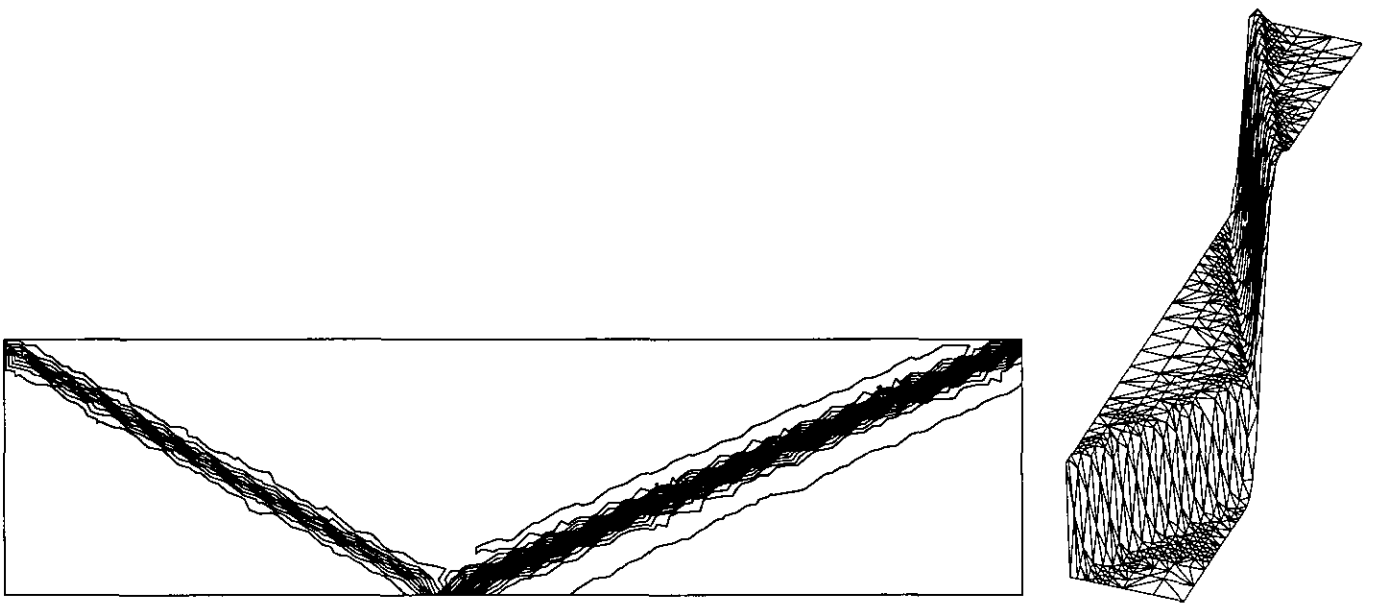

FIG. 11. Viscosity matrix C_A, triangular elements.

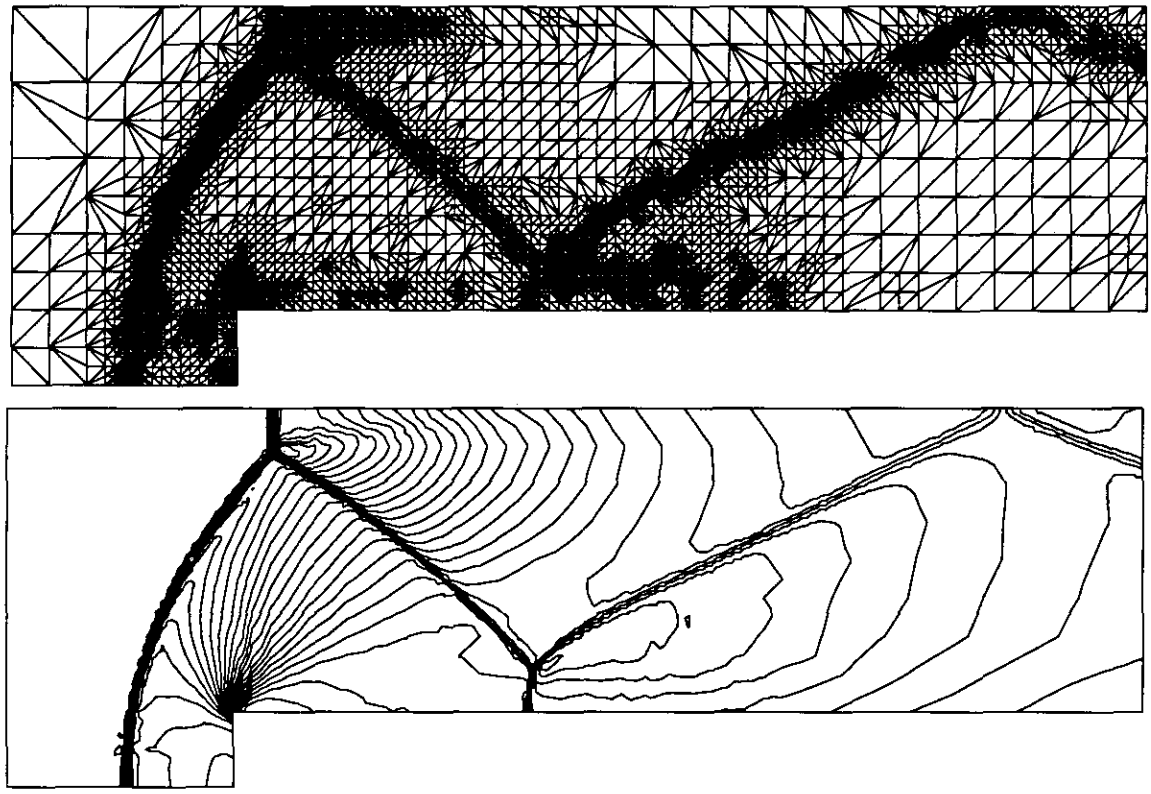

FIG. 12. Mesh and density, viscosity matrix C_n.

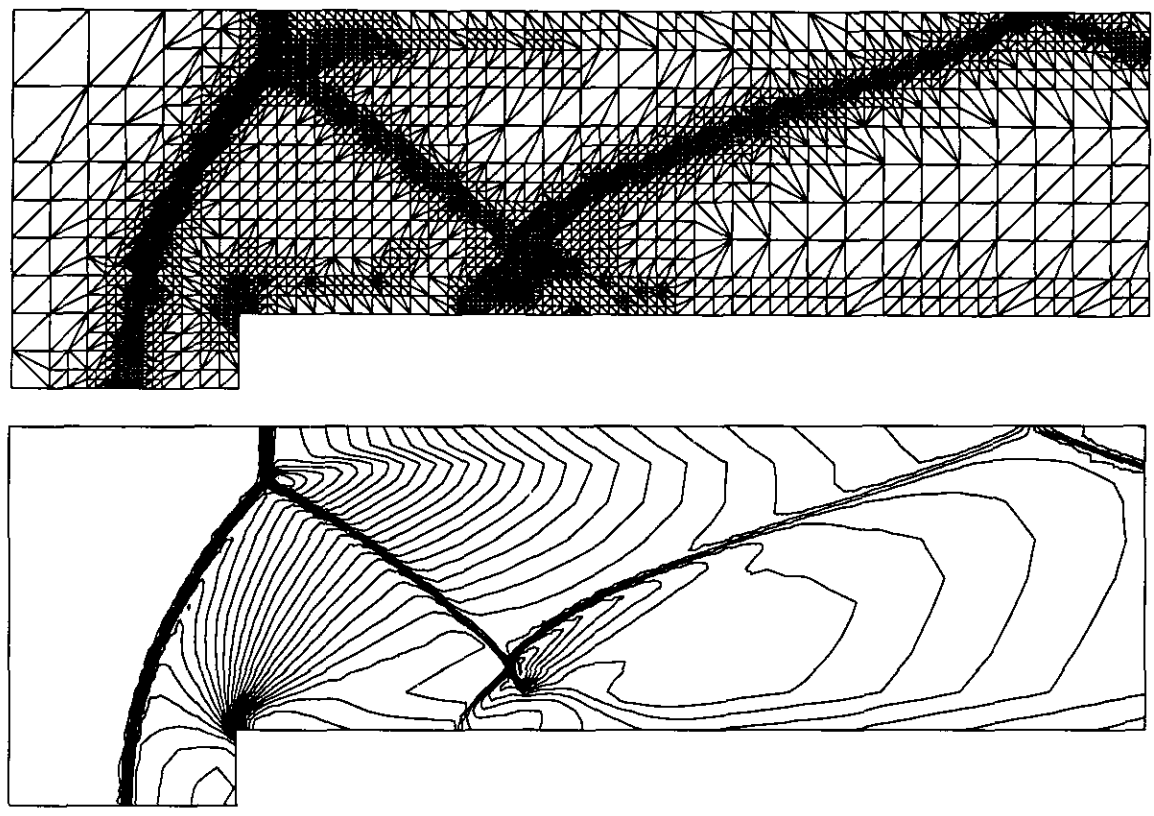

FIG. 13. Mesh and density, viscosity matrix C_A.

where $\mathbf{n}$ is normal to the element side. Note the excessive smearing obtained with this choice as well as with $\mathbf{C}_n^*$ in the case of square elements (Fig. 6). The results using the approximate diagonalization approach have been stabilized with artificial viscosity.

Note the slight instability using the directionally biased approach which is more pronounced for bilinear elements. This may perhaps be remedied by using another definition of $\mathbf{n}$ (note, e.g., that Davis [19] did not use the pressure, but differences in velocity), but that question is beyond the scope of the present work.

Wind Tunnel with a Step

This classical example consists of a wind tunnel of height one unit and length three units. The step is 0.2 units high and positioned 0.6 units from the left-hand inflow entrance of the tunnel. The initial data consists of a Mach 3 flow with $\mathbf{U} = (1.4, 4.2, 0, 8.8)$; these values are also prescribed at the inflow entrance. No special attention has been devoted to the singularity at the corner of the step. Again, the adaptive algorithm described in [7] has been employed. The mesh and density isolines are shown at time $t = 3$ for the directionally biased (Fig. 12) and approximate diagonalization approaches (Fig. 13). The latter shows a better resolution of the contact discontinuity leaving the Mach stem at the ceiling. The spurious Mach stems at the floor are (to some extent) caused by the non-treatment of the singularity at the corner of the step, see Woodward and Colella [24].

6. CONCLUSIONS

In this paper we have shown the flexibility of the streamline diffusion finite element method applied to the Eulerian equations of fluid dynamics. In particular, the relation to several of the finite difference and finite volume upstream methods has been shown, and also the relation to Lax–Wendroff type methods. On the one hand, new (and old) choices of upwind directions, which take into account the structure of the solution, may easily be incorporated. On the other hand, a particular choice of upwinding which does not hinge on directionality has been devised and shown to give good results. Furthermore, we have discussed the basic entropy stability obtained with the method, and how this stability relates to the choice of weighting functions when conservation variables are used.

Regarding computational speed, it is clear that the SD-method with an explicit implementation can be as fast as a typical finite difference method on a structured mesh, assuming that the implementation takes into account the structure of the mesh. The typical FEM-implementation is made for unstructured meshes, however, and there is thus an inherently time-consuming additional complexity in FEM. This is the price for the increasing applicability of the method; it should be considered a small price to pay.

APPENDIX

The Euler equations in two dimensions may be written in quasi-linear form

$$\frac{\partial \mathbf{u}}{\partial t} + \sum_{i=1}^{2} \mathbf{A}_i \frac{\partial \mathbf{u}}{\partial x_i} = 0,$$

where

$$\mathbf{u} = \varrho \begin{bmatrix} 1 \\ u_1 \\ u_2 \\ e \end{bmatrix}, \qquad \mathbf{A}_i = \frac{\partial \mathbf{f}_i}{\partial \mathbf{u}}$$

and

$$\mathbf{f}_i = u_i \mathbf{u} + p \begin{bmatrix} 0 \\ \delta_{1i} \\ \delta_{2i} \\ u_i \end{bmatrix}.$$

Here, ϱ is the density, u_i is the velocity, e is the total energy density, $p = (\gamma - 1)(\varrho e - \varrho(u_1^2 + u_2^2)/2)$ is the pressure, and δ_{ij} is the Kronecker delta.

Directional Case

Define a matrix $\mathbf{A}_n = \mathbf{A}_1 n_1 + \mathbf{A}_2 n_2$, where n_1 and n_2 are real numbers, and let $c = (\gamma p/\varrho)^{1/2}$, $\bar{\gamma} = \gamma - 1$, $\mathbf{n} = (n_1, n_2)$, and $\mathbf{q} = (u_1, u_2)$. The eigenvalues, the eigenvectors, and the inverse of the eigenvectors of $\mathbf{A}_n$ are given by:

- Eigenvalues,

$$\begin{bmatrix} \mathbf{n}\cdot\mathbf{q} \\ \mathbf{n}\cdot\mathbf{q} \\ \mathbf{n}\cdot\mathbf{q} - c\,|\mathbf{n}| \\ \mathbf{n}\cdot\mathbf{q} + c\,|\mathbf{n}| \end{bmatrix}$$

- Eigenvectors,

$$\begin{bmatrix} 1 & 0 & c^{-2} & c^{-2} \\ u_1 & -\dfrac{n_2\varrho}{n_1} & -\dfrac{n_1}{c\,|\mathbf{n}|} + \dfrac{u_1}{c^2} & \dfrac{n_1}{c\,|\mathbf{n}|} + \dfrac{u_1}{c^2} \\ u_2 & \varrho & -\dfrac{n_2}{c\,|\mathbf{n}|} + \dfrac{u_2}{c^2} & \dfrac{n_2}{c\,|\mathbf{n}|} + \dfrac{u_2}{c^2} \\ \dfrac{|\mathbf{q}|^2}{2} & -\dfrac{n_2\varrho u_1}{n_1} + \varrho u_2 & \dfrac{1}{\bar{\gamma}} - \dfrac{\mathbf{n}\cdot\mathbf{q}}{c\,|\mathbf{n}|} + \dfrac{|\mathbf{q}|^2}{2c^2} & \dfrac{1}{\bar{\gamma}} + \dfrac{\mathbf{n}\cdot\mathbf{q}}{c\,|\mathbf{n}|} + \dfrac{|\mathbf{q}|^2}{2c^2} \end{bmatrix}$$

- Inverse,

$$\begin{bmatrix} 1-\frac{\bar\gamma|\mathbf{q}|^2}{2c^2} & \frac{\bar\gamma u_1}{c^2} & \frac{\bar\gamma u_2}{c^2} & -\frac{\bar\gamma}{c^2} \\ -\frac{n_1(n_1u_2-n_2u_1)}{\varrho|\mathbf{n}|^2} & -\frac{n_1n_2}{\varrho|\mathbf{n}|^2} & \frac{n_1^2}{\varrho|\mathbf{n}|^2} & 0 \\ \frac{c\mathbf{n}\cdot\mathbf{q}}{2|\mathbf{n}|}+\frac{\bar\gamma|\mathbf{q}|^2}{4} & -\frac{cn_1}{2|\mathbf{n}|}-\frac{\bar\gamma u_1}{2} & -\frac{cn_2}{2|\mathbf{n}|}-\frac{\bar\gamma u_2}{2} & \frac{\bar\gamma}{2} \\ -\frac{c\mathbf{n}\cdot\mathbf{q}}{2|\mathbf{n}|}+\frac{\bar\gamma|\mathbf{q}|^2}{4} & \frac{cn_1}{2|\mathbf{n}|}-\frac{\bar\gamma u_1}{2} & \frac{cn_2}{2|\mathbf{n}|}-\frac{\bar\gamma u_2}{2} & \frac{\bar\gamma}{2} \end{bmatrix}$$

Approximate Diagonalisation

We now turn to the matrix $\mathbf{C}=\mathbf{A}_1^2+\mathbf{A}_2^2$. Let $\tilde c=(c^2+16u_1^2+16u_2^2)^{1/2}$. Then the eigenvalues, the eigenvectors, and the inverse of the eigenvectors of $\mathbf{C}$ are given by:

- Eigenvalues,

$$\begin{bmatrix} |\mathbf{q}|^2 \\ |\mathbf{q}|^2+c^2 \\ |\mathbf{q}|^2+\frac{3c^2}{2}-\frac{c\tilde c}{2} \\ |\mathbf{q}|^2+\frac{3c^2}{2}+\frac{c\tilde c}{2} \end{bmatrix}$$

- Eigenvectors,

$$\begin{bmatrix} 1 & 0 & c^{-2} & c^{-2} \\ u_1 & -\frac{\varrho u_2}{u_1} & \frac{u_1}{c^2}+\frac{4u_1}{c^2-c\tilde c} & \frac{u_1}{c^2}+\frac{4u_1}{c^2+c\tilde c} \\ u_2 & \varrho & \frac{u_2}{c^2}+\frac{4u_2}{c^2-c\tilde c} & \frac{u_2}{c^2}+\frac{4u_2}{c^2+c\tilde c} \\ \frac{|\mathbf{q}|^2}{2} & 0 & \frac{1}{\bar\gamma}+\frac{|\mathbf{q}|^2}{2c^2}+\frac{4|\mathbf{q}|^2}{c^2-c\tilde c} & \frac{1}{\bar\gamma}+\frac{|\mathbf{q}|^2}{2c^2}+\frac{4|\mathbf{q}|^2}{c^2+c\tilde c} \end{bmatrix}$$

- Inverse,

$$\begin{bmatrix} 1-\frac{\bar\gamma|\mathbf{q}|^2}{2c^2} & \frac{\bar\gamma u_1}{c^2} & \frac{\bar\gamma u_2}{c^2} & -\frac{\bar\gamma}{c^2} \\ 0 & -\frac{u_1u_2}{\varrho|\mathbf{q}|^2} & \frac{u_1^2}{\varrho|\mathbf{q}|^2} & 0 \\ \frac{2c|\mathbf{q}|^2}{\tilde c}+\frac{4\bar\gamma|\mathbf{q}|^4}{\tilde c^2+c\tilde c} & \frac{-2cu_1}{\tilde c}-\frac{8\bar\gamma u_1|\mathbf{q}|^2}{\tilde c^2+c\tilde c} & \frac{-2cu_2}{\tilde c}-\frac{8\bar\gamma u_2|\mathbf{q}|^2}{\tilde c^2+c\tilde c} & \frac{8\bar\gamma|\mathbf{q}|^2}{\tilde c^2+c\tilde c} \\ -\frac{2c|\mathbf{u}|^2}{\tilde c}+\frac{4\bar\gamma|\mathbf{q}|^4}{\tilde c^2-c\tilde c} & \frac{2cu_1}{\tilde c}+\frac{8\bar\gamma u_1|\mathbf{q}|^2}{-\tilde c^2+c\tilde c} & \frac{2cu_2}{\tilde c}+\frac{8\bar\gamma u_2|\mathbf{q}|^2}{-\tilde c^2+c\tilde c} & -\frac{8\bar\gamma|\mathbf{q}|^2}{-\tilde c^2+c\tilde c} \end{bmatrix}$$

REFERENCES

1. T. J. R. Hughes and T. E. Tezduyar, *Comput. Methods Appl. Mech. Engrg.* **45**, 217 (1984).
2. T. J. R. Hughes and M. Mallet, *Comput. Methods Appl. Mech. Engrg.* **58**, 305 (1986).
3. F. Shakib, T. J. R. Hughes, and Z. Johan, *Comput. Methods Appl. Mech. Engrg.* **89**, 141 (1991).
4. P. Hansbo, C. Johnson, and A. Szepessy, in *Proceedings, 7th Int. Conf. on Finite Element Methods in Flow problems, Huntsville, 1989*, edited by T. J. Chung and G. R. Karr (UAH Press, Huntsville, 1989), p. 377.
5. C. Johnson, A. Szepessy, and P. Hansbo, *Math. Comput.* **54**, 107 (1990).
6. A. Szepessy, Ph.D. thesis, Department of Mathematics, Chalmers University of Technology, 1989 (unpublished).
7. P. Hansbo and C. Johnson, *Comput. Methods Appl. Mech. Engrg.* **87**, 267 (1991).
8. T. J. R. Hughes, L. P. Franca, and M. Mallet, *Comput. Methods Appl. Mech. Engrg.* **54**, 223 (1986).
9. M. S. Mock, *J. Differential Equations* **37**, 70 (1980).
10. A. Harten, *J. Comput. Phys.* **49**, 151 (1983).
11. E. Tadmor, *Math. Comput.* **49**, 91 (1987).
12. B. Van Leer, *J. Comput. Phys.* **23**, 263 (1977).
13. S. Osher and F. Solomon, *SIAM J. Numer. Anal.* **38**, 339 (1982).
14. J. L. Steger and R. F. Warming, *J. Comput. Phys.* **40**, 263 (1981).
15. G. Vijayasundaram, *J. Comput. Phys.* **63**, 416 (1986).
16. R. Löhner, K. Morgan, and O. C. Zienkiewicz, *Int. J. Numer. Methods Fluids* **4**, 1043 (1984).
17. A. Harten, P. D. Lax, and B. Van Leer, *SIAM Rev.* **25**, 35 (1983).
18. R. F. Warming, R. M. Beam, and B. J. Hyett, *Math. Comput.* **29**, 1037 (1975).
19. S. F. Davis, *J. Comput. Phys.* **56**, 65 (1984).
20. L. Fezoui and B. Stoufflet, *J. Comput. Phys.* **84**, 174 (1989).
21. S. Osher, *C.R. Acad. Sci. Paris Ser. A* **290**, 819 (1980).
22. B. Cockburn, S. Hou, and C.-W. Shu, *Math. Comput.* **54**, 545 (1990).
23. G. A. Sod, *J. Comput. Phys.* **27**, 1 (1978).
24. P. Woodward and P. Colella, *J. Comput. Phys.* **54**, 115 (1984).